Modelling an industrial anaerobic granular reactor using a multi-scale approach

Feldman, Hannah; Flores Alsina, Xavier; Ramin, Pedram; Kjellberg, K.; Jeppsson, U.; Batstone, Damien J.; Gernaey, Krist V.

Published in:
Water Research

Link to article, DOI:
10.1016/j.watres.2017.09.033

Publication date:
2017

Document Version
Peer reviewed version

Accepted Manuscript

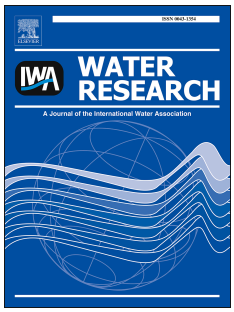

Modelling an industrial anaerobic granular reactor using a multi-scale approach

H. Feldman, X. Flores-Alsina, P. Ramin, K. Kjellberg, U. Jeppsson, D.J. Batstone, K.V. Gernaey

PII: S0043-1354(17)30780-7

DOI: 10.1016/j.watres.2017.09.033

Reference: WR 13227

To appear in: *Water Research*

Received Date: 21 June 2017

Revised Date: 12 September 2017

Accepted Date: 13 September 2017

Please cite this article as: Feldman, H., Flores-Alsina, X., Ramin, P., Kjellberg, K., Jeppsson, U., Batstone, D.J., Gernaey, K.V., Modelling an industrial anaerobic granular reactor using a multi-scale approach, *Water Research* (2017), doi: 10.1016/j.watres.2017.09.033.

GRAPHICAL ABSTRACT

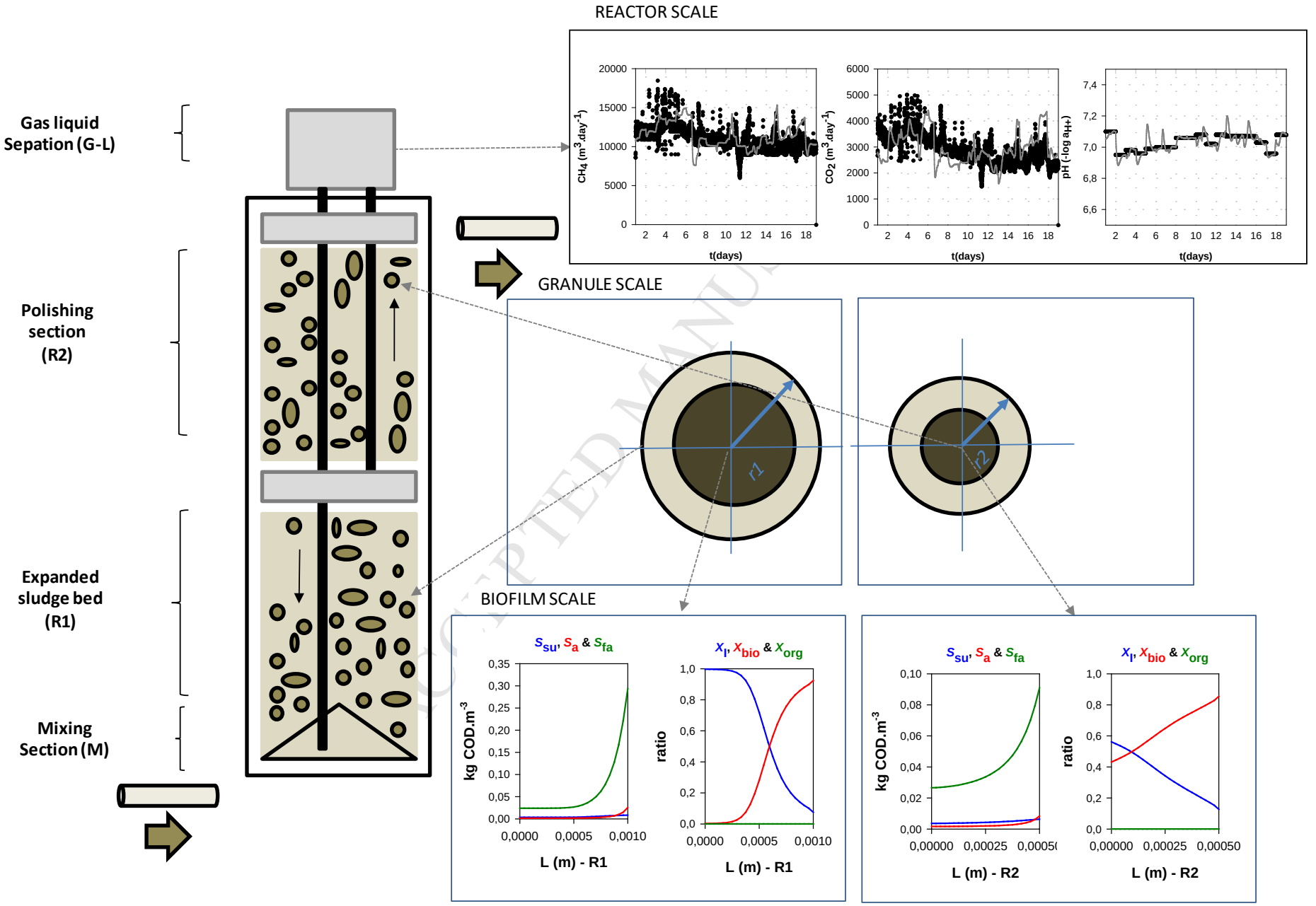

Modelling an industrial anaerobic granular reactor using a multi-scale approach

H. Feldman[1], X. Flores-Alsina[1], P. Ramin[1], K. Kjellberg[2], U. Jeppsson[3], D.J. Batstone[4], K.V. Gernaey[1]

[1] Process and Systems Engineering Center (PROSYS), Department of Chemical and Biochemical Engineering, Technical University of Denmark, Building 229, DK-2800 Kgs. Lyngby, Denmark.

[2] Novozymes A/S, Hallas Alle 1, DK-4400 Kalundborg, Denmark.

[3] Division of Industrial Electrical Engineering and Automation, Department of Biomedical Engineering, Lund University, Box 118, SE-221 00 Lund, Sweden.

[4] Advanced Water Management Centre (AWMC), The University of Queensland, St Lucia, Brisbane, Queensland 4072 Australia.

ABSTRACT

The objective of this paper is to show the results of an industrial project dealing with modelling of anaerobic digesters. A multi-scale mathematical approach is developed to describe reactor hydrodynamics, granule growth/distribution and microbial competition/inhibition for substrate/space within the biofilm. The main biochemical and physico-chemical processes in the model are based on the Anaerobic Digestion Model No 1 ($ADM1$) extended with the fate of phosphorus (P), sulfur (S) and ethanol ($Et-OH$). Wastewater dynamic conditions are reproduced and data frequency increased using the Benchmark Simulation Model No 2 ($BSM2$) influent generator. All models are tested using two plant data sets corresponding to different operational periods ($\#D1, \#D2$). Simulation results reveal that the proposed approach can satisfactorily describe the transformation of organics, nutrients and minerals, the production of methane, carbon dioxide and sulfide and the potential formation of precipitates within the bulk (average deviation between computer simulations and measurements for both $\#D1, \#D2$ is around 10 %) Model predictions suggest a stratified structure within the granule which is the result of: 1) applied loading rates, 2) mass transfer limitations and 3) specific (bacterial) affinity for substrate. Hence, inerts (X_{I}) and methanogens (X_{ac}) are situated in the inner zone, and this fraction lowers as the radius increases favouring the presence of acidogens ($X_{\mathrm{su}}, X_{\mathrm{aa}}$, X_{fa}) and acetogens ($X_{\mathrm{c4}}, X_{\mathrm{pro}}$). Additional simulations show the effects on the overall process performance

when operational (pH) and loading ($S:COD$) conditions are modified. Lastly, the effect of intra-granular precipitation on the overall organic/inorganic distribution is assessed at: 1) different times; and, 2) reactor heights. Finally, the possibilities and opportunities offered by the proposed approach for conducting engineering optimization projects are discussed.

KEYWORDS

ADM1, Bacterial Competition, Biofilms, Industrial Wastewater, Sulfate Reducing Bacteria, Physico-Chemical Modelling.

NOMENCLATURE

AD	Anaerobic digestion
ADM1	Anaerobic Digestion Model No 1
AFBR	Anaerobic fluidized bed reactor
AT	Anaerobic technologies
BSM2	Benchmark Simulation Model No 2
CH_4	Methane production measurements ($m^3.day^{-1}$)
CSTR	Continuous stirred tank reactor
CO_2	Carbon dioxide production measurements ($m^3.day^{-1}$)
COD	Chemical oxygen demand
$\#D$	Data set for model testing
DA	Degree of acidification
Et-OH	Ethanol
EGSB	Expanded granular sludge bed
$G-L$	Gas liquid separation unit
$G_{\mathrm{CH_4}}$	Methane production rate (model) (gas) (ADM1) ($m^3.day^{-1}$)
$G_{\mathrm{CO_2}}$	Carbon dioxide production rate (model) (gas) (ADM1) ($m^3.day^{-1}$)
$G_{\mathrm{H_2}}$	Hydrogen production rate (gas) (model) (ADM1) ($m^3.day^{-1}$)
$G_{\mathrm{H_2S}}$	Hydrogen sulfide production rate (model) (gas) (ADM1) ($m^3.day^{-1}$)
H_2S	Sulfide production measurements ($m^3.day^{-1}$)
$H_xPO_4^{3-x}$	Phosphate measurements ($g.m^{-3}$)
IC	Internal circulation
L	Biofilm thickness (m)
N	Nitrogen
$N_{\mathrm{organic.s}}$	Nitrogen soluble measurements ($g.m^{-3}$)
$N_{\mathrm{organic.p}}$	Nitrogen particulate measurements ($g.m^{-3}$)
NH_x	Ammonium/ammonia measurements ($g.m^{-3}$)
M	Mixing section
MET	Methanogenic bacteria

MMP	Multiple mineral precipitation
P	Phosphorus
$R1$	Expanded sludge bed section of the reactor
$R2$	Polishing section of the reactor
S	Soluble compound (model)
SI	Saturation index
SO_x^{2-}	Sulfate/sulfite measurements ($g.m^{-3}$)
SRB	Sulfate reducing bacteria
S_{aa}	Amino acids (ADM1) ($kg\ COD.m^{-3}$)
S_{ac}	Total acetic acid (ADM1) ($kg\ COD.m^{-3}$)
$S_{biomass}$	S content in biomass (ADM1) ($kmol\ S.kg\ COD.m^{-3}$)
S_{bu}	Total butyric acid (ADM1) ($kg\ COD.m^{-3}$)
S_{Ca}	Calcium (ADM1) ($kmol.m^{-3}$)
S_{Cl}	Chloride (ADM1) ($kmol.m^{-3}$)
S_{Et-OH}	Ethanol (ADM1) ($kmol.m^{-3}$)
S_{fa}	Fatty acids (ADM1) ($kg\ COD.m^{-3}$)
S_{H_2}	Hydrogen (ADM1) ($kg\ COD.m^{-3}$)
S_{IC}	Inorganic carbon (ADM1) ($kmol.m^{-3}$)
S_{IN}	Inorganic nitrogen (ADM1) ($kmol.m^{-3}$)
S_{IP}	Inorganic phosphorus (ADM1) ($kmol.m^{-3}$)
S_{IS}	Inorganic total sulfides (ADM1) ($kg\ COD.m^{-3}$)
S_K	Potassium (ADM1) ($kmol.m^{-3}$)
S_{Mg}	Magnesium (ADM1) ($kmol.m^{-3}$)
S_{Na}	Sodium (ADM1) ($g.m^{-3}$) ($kmol.m^{-3}$)
S_{pro}	Total propionic acid (ADM1) ($kg\ COD.m^{-3}$)
S_{prot}	Sulfur in proteins (ADM1) ($kmol.kgCOD^{-1}$)
S_{su}	Sugars (ADM1) ($kg\ COD.m^{-3}$)
S_{SO_4}	Sulfate (ADM1) ($kmol.m^{-3}$)
S_{va}	Total valeric acid (ADM1) ($kg\ COD.m^{-3}$)
TKN	Total Kjeldahl nitrogen measurements ($g.m^{-3}$)
TN	Total nitrogen measurements ($g.m^{-3}$)
TP	Total phosphorus measurements ($g.m^{-3}$)
TSS	Total suspended solids measurements ($g.m^{-3}$)
UASB	Upflow anaerobic sludge blanket
VFA	Volatile fatty acids measurements ($g.m^{-3}$)
V_{Gas}	Gas volume in the bioreactor
V_{Liq}	Liquid volume in the bioreactor
WRRF	Water resource recovery facility
WWTP	Wastewater treatment plant
X_{ac}	Particulate compound
X_{ac}	Acetate degraders (ADM1) ($kg\ COD.m^{-3}$)
$X_{BIOMASS}$	Total biomass (ADM1) ($kg\ COD.m^{-3}$)
X_{C4}	Butyrate and valerate degraders (ADM1) ($kg\ COD.m^{-3}$)

X_{CaCO_3}	Calcite (ADM1) (kmol.m^{-3})
X_{ch}	Carbohydrates (ADM1) (kg COD.m^{-3})
X_{Et-OH}	Ethanol degraders (ADM1) (kg COD.m^{-3})
X_{I}	Inert particulate organics (ADM1) (kg COD.m^{-3})
X_{li}	Lipids (ADM1) (kg COD.m^{-3})
X_{pr}	Proteins (ADM1) (kg COD.m^{-3})
X_{pro}	Propionate degraders (ADM1) (kg COD.m^{-3})
X_{SRB}	Sulfate reducing bacteria (ADM1) (kg COD.m^{-3})
z	Radial distance within the biofilm (m)
Z_i	Chemical species concentration of species i (algebraic variable of the physico-chemistry module) (kmol.m^{-3})

1. INTRODUCTION

Resource recovery from wastewater processes is a rapidly emerging research area, which has promoted the development of different types of anaerobic technologies (AT) (amongst others) as a sustainable way to treat highly loaded domestic and industrial wastewaters (**Batstone et al., 2015**). The reason is mainly that anaerobic systems can: 1) ensure compliance with the effluent discharge limits; 2) produce biogas that can be converted to energy (heat/electricity) to reduce the power demands within the treatment facility; and, 3) avoid nutrient destruction and enables its potential capture in different forms and qualities (**Tchobanoglous *et al.*, 2003**). Therefore, engineering practice is facing a transition from conventional wastewater treatment plants ($WTTPs$) into water resource recovery facilities ($WRRFs$) (**Daigger *et al.*, 2011**).

Mathematical models have demonstrated to be highly effective for benchmarking (**Copp, 2002; Jeppsson *et al.*, 2007**), diagnosis (**Rodriguez-Roda *et al.*, 2002**), design (**Flores-Alsina *et al*, 2012, Benedetti *et al.*, 2010**), teaching (**Hug *et al.*, 2009**) and optimization (**Rivas *et al.*, 2008**) of $WRRFs$. Since the publication of the International Water Association (IWA) Anaerobic Digestion Model No 1 ($ADM1$) (**Batstone *et al.*, 2002**) the field of has been rapidly expanding. Numerous studies presenting new technologies, new processes and the need to consider anaerobic systems in a much broader context of the wastewater cycle as a whole have been published in specialized literature (**Batstone *et al.*, 2015**). However, practical applications of these models, and particularly industrial cases, have been relatively limited. A potential reason for this is that commercial software applications (e.g. GPS-X, WEST-DHI, SUMO, BIOWIN, EFOR, SIMBA) including state-of-the-art mathematical models (**Henze *et al.*, 2000; Batstone *et al.*, 2002**) were originally

developed to predict the performance of urban wastewater systems treating domestic wastewater, and therefore fail to properly represent specific industrial processes.

Industrial wastewaters have very diverse dynamics (compared to urban wastewater), which is a result of different production schemes/schedules within the factory (**Gernaey *et al.*, 2011)**. Variable pH (**Fang *et al.*, 2002**), influent biodegradability (**Astals *et al.*, 2013**), non-standard $N:COD$ and $P:COD$ ratios (**Punal *et al.*, 2000**) might challenge traditional biological processes. In some cases, high S loads decrease methane/biogas production (and potential energy recovery) (**Tchobanoglous *et al.*, 2003**). This reduction is attributed to two factors: 1) loss of electron equivalents due to sulfate reducing bacteria (**Hao *et al.*, 2014, Liu et al., 2015a,b**); and, 2) decrease of acetoclastic and hydrogenotrophic methanogenesis due to sulfide inhibition (**Kalyuzhnyi and Fedorovich, 1998**). Metals and some inorganic/organic compounds can inhibit microorganism growth and/or have severe toxicity effects (**Chen *et al.*, 2008**). The high content of cations and anions promotes the formation of precipitates at different locations in the reactor (granules, pipes), which can have detrimental (decrease of methanogenic activity) or catastrophic (cementation) effects on reactor performance (**Van Langerak *et al.* 1998; 2000**). Hence, mathematical models describing industrial wastewater reactors should include all these (hostile) phenomena in order to produce reliable predictions.

Another important factor to account for among the modelling challenges when representing high rate configurations, which are widely used in industry, such as upflow anaerobic sludge blanket reactors ($UASB$), expanded granular sludge bed ($EGSB$) reactors or anaerobic fluidized bed reactors ($AFBR$) (**Saravanann and Sreekrishnan, 2006**), is the multi-scale concept. In such systems, processes occur at very different spatial (from mm to m) and temporal scales (from seconds to days) (**Wanner *et al.*, 2006; Xavier *et al.*, 2005)**. For example, acid-base reactions are very fast, while microbial growth is rather slow. Such slow and fast variations causes well-known numerical stiffness problems and hence special solvers are necessary **(Flores-Alsina *et al.*, 2015**). This can be critical when the modelling is to be used for control using rigorous sensor and actuator models (**Rosen *et al.*, 2008**). At reactor scale, the effects of the hydrodynamics on the overall process performance should be included (**Batstone *et al.*, 2005**). In systems where microorganisms are anchored into granules, their structure, size and distribution within the reactor must be taken into account since these have strong effects on the overall process performance (**Volcke *et al.*, 2010; 2012**). Finally, a third scale to consider is the microbial metabolism along with transport of soluble (diffusion) and particulate

(convection) compounds (**Van Lier *et al.*, 2015**). These processes will govern the spatial location of the particulate compounds, such as the bacteria, inert material and other particulates, e.g. precipitates (**Rittmann and McCarty, 1980**; **Boltz *et al.*, 2011**). At present, most of the full-scale modelling studies dealing with high rate anaerobic systems have not taken all these aspects (full-scale, multi-scale, N, P & S, multiple mineral precipitation) into account simultaneously (**Batstone and Keller, 2003; Batstone *et al.*, 2004a; Erashin *et al.*, 2007; Chen *et al.*, 2009; Dereli *et al.*, 2010; Hinken *et al.*, 2014; Aymerich *et al.*, 2015, Barrera *et al.*, 2015**). As a consequence, it is not possible to properly describe liquid, gas and granule transport processes, including liquid to granule and liquid to gas transfer or inter-granule mass transfer limitations and inter-granule heterogeneity (**Wanner *et al.*, 2006**).

In order to circumvent these limitations, the objective of this paper is to develop a multi-scale (reactor, granule, biofilm) approach for mechanistic description of the main biological and physico-chemical processes taking place in industrial anaerobic granular reactors. At the *biofilm* level, special emphasis is placed on describing the competition between sulfate reducing bacteria and methanogens, the addition of ethanol as a separate model component, the effect of ionic strength/activity corrections and the formation of multiple mineral precipitates. Flow patterns, granular distribution and size are addressed at *reactor* and *granular* level, respectively. The proposed approach is experimentally tested using two different data sets corresponding to different operational modes. In addition, for this case study the authors have developed: 1) a phenomenological approach to increase data frequency and therefore providing additional dynamics to influent data; and, 2) a statistical (inference) method for parameter estimation. The paper details the development of the new model by presenting sequentially the elements of which it is comprised as well as highlighting the integration/interfacing aspects. The capabilities/potentials of the proposed approach are illustrated by several simulated scenario analyses. Lastly, opportunities and limitations that arise from utilization of the new model are discussed.

2. METHODS

2.1. Plant configuration

The plant under study is located in Kalundborg - North Western part of Zealand (Denmark). Reactor design is based on the BIOPAQ®IC technology (Paques, the Netherlands), a special version of the *EGSB* concept.

In general, $EGSB$ systems employ granular sludge, which is characterized by high mass transfer area, high volumetric conversion rates and ultimately enabling more compact installations (**Van Lier *et al.*, 2015**). The latter ensures a higher energy recovery potential compared to traditional digestion systems. The reactor is comprised of four parts: 1) a mixing section (M); 2) an expanded sludge bed ($R1$); 3) a polishing section ($R2$); and, 4) a gas-liquid separator ($G-L$). In M the influent is evenly distributed within the reactor. The water flows upwards to $R1$ where most of the organic pollutants are converted into biogas. The effective contact between water and granular anaerobic biomass allows for a higher load. Next, the biogas produced is collected in the lower separation module and flows upwards through the riser to $G-L$ at the top of the reactor. In this section, the water and biogas are separated. The water flows into the downer to the bottom, and it is mixed with the influent. This flow of water from $R1$ through the riser and the downer and back into M is called the internal circulation (IC) and it gives the reactor its name. In fact, the lifting forces of the collected biogas are used to bring about the IC of the liquid (and granular sludge) over $R1$. The water from $R1$ flows to the upper compartment ($R2$), which has a lower organics concentration. In this section, the rest of the organic material is transformed into biogas. This biogas flows upwards to the headspace, while water is sent to M through the downer or leaves the reactor with the overflow. The biogas leaves the reactor at the top and the polished effluent through the effluent pipe (see **Figure 1** for details).

2.2. Data measuring campaign

Two different data sets ($\#D1$, $\#D2$) corresponding to two operational periods are used to test the predictive capabilities of the model. For the first data set ($\#D1$) (from 25.01.2016 to 11.02.2016) the influent flow rate/mass loadings into the industrial AD are 144 $m^3.h^{-1}$, 1600 kg $COD.h^{-1}$, 70 kg $N.h^{-1}$ and 40 kg $P.h^{-1}$. The influent $S{:}COD$ ratio is 0.025 kg S.kg COD^{-1}. Data for the second period ($\#D2$) (from 28.08.2016 to 19.09.2016) show higher $N{:}COD$ and lower $P{:}COD$ ratios, higher protein concentration, more precipitates and a higher degree of acidification (DA). In absolute values, flow rate/mass loadings into the industrial AD are 207 $m^3.h^{-1}$, 2 200 kg $COD.h^{-1}$, 160 kg $N.h^{-1}$ and 35 kg $P.h^{-1}$. The influent $S{:}COD$ ratio remains almost the same (0.027 kg S.kg COD^{-1}). Samples are taken at the outlet of the pre-acidification tank ($PreAD$), a unit before the studied anaerobic granular bioreactor to promote the growth fermenters and formation of VFA. Rigorous mass balances are conducted to: 1) characterize influent fractions; and, 2) check data quality

(see Tables S1-S5 in the Supplemental Information section). It is important to highlight that influent conditions are extremely variable since the system under investigation treats the wastewater from two large biotech industries (Novozymes and Novo-Nordisk) located in the NW part of Zealand, Denmark. Indeed, wastewater composition strongly depends on production schedules, which change over the year. For both periods, data on influent/effluent cations (Na^+, K^+, Ca^{+2}, Mg^{+2}) and anions (Cl^-, SO_x^{-2},) are available. Analyses were done using Standard Methods (APHA, 2012) using 1 day composite samples. H_2S in the aqueous phase are grab samples as the sulfides are so volatile it is not accurate to take a composite measurements. In addition, pH, CH_4, CO_2, H_2S, VFA and $alkalinity$ were continuously measured inside the reactor (5 min frequency).

2.3. Influent generation

The model blocks for: 1) flow-rate generation ($FLOW$); 2) compounds generation ($POLLUTION$); and, 3) sewer network ($TRANSPORT$), developed for the Benchmark Simulation Model No 2 ($BSM2$) (**Gernaey *et al.*, 2011)** influent generator, are used to reproduce the wastewater dynamics. The BSM2 influent generator is developed for urban wastewater but can also be applied to industrial systems. The main idea behind this model is to assume specific (daily/weekly) industry-type defined profiles ($FLOW$, $POLLUTION$), which are sampled cyclically and combined by multiplication. The resulting output (averaged to 1) is scaled to the desired influent conditions assuming specific loading rates. Based on the available measurements, the $BSM2$ influent generator provides: 1) additional influent dynamics; 2) increased data frequency; and, 3) a more realistic and complete picture of how the $WTTP$ might perform under a wide range of disturbances (**Flores-Alsina *et al.*, 2014; Snip *et al.*, 2016**).

2.4. (Bio) chemical model

Reaction rates in both bulk and biofilm are evaluated using the stoichiometry and kinetics as described in the $ADM1$ (**Batstone *et al.*, 2002**). The operational temperature is constant at 35°C (mesophilic conditions). The default implementation is upgraded to include P, S and ethanol ($Et-OH$) related conversion processes (**Flores-Alsina *et al.*, 2016**). P is modelled using a source-sink approach assuming a predefined elemental (C, H, N, P, O) composition (**de Gracia *et al.*, 2006**). Biological production of sulfides (S_{IS}) is described by means of sulfate reducing bacteria (X_{SRB}) utilising hydrogen (S_{H_2}) (autolithotrophically) as electron donor

(**Batstone, 2006**). Potential hydrogen sulfide (Z_{H_2S}) inhibition and stripping of H_2S to the gas phase (G_{H_2S}) are considered (**Federovich *et al.*, 2003**). Finally, $Et-OH$ (S_{EtOH}) degradation is modelled assuming a specific group of microorganisms (X_{EtOH}), which end up producing hydrogen (S_{H_2}) and acetate (S_{ac}) (**Batstone *et al.*, 2004b**). Since the ΔG values and stoichiometry of hydrogen production are similar for ethanol and butyrate degraders, the default kinetic parameters and S_{H_2} inhibition parameters for butyrate degraders (X_{c4}) were used as starting values to describe S_{EtOH} degradation (**Batstone *et al.*, 2004b**). The model also includes physico-chemical equations that simulate the acid-base system and thereby pH (**Solon *et al.*, 2015a**). The model corrects for ionic strength via the Davies approach to consider chemical activities instead of molar concentrations and hence perform all the calculations under non-ideal conditions (**Flores-Alsina *et al.*, 2015**). Multiple mineral precipitation is based on Saturation Index calculations (SI) as stated in **Kazadi Mbamba *et al.* (2015a;b).**

2.5. Multi-scale reactor model

A multi-scale, fully-coupled modelling approach is adopted to describe the system under study (see **Figure 1**). At *reactor scale,* $R1$ and $R2$ are modelled as a series of continuous stirred tank reactors ($CSTR$). The bottom compartment (R1) is comprised mainly of the sludge bed, and the top compartment (R2) act as polisher and has a low biomass concentration. Each $CSTR$ contains a liquid (V_{Liq}) and a gas phase (V_{Gas}) volume in order to take into account mass transfer phenomena. The total liquid (V_{Liq}) and gas phase (V_{Gas}) volumes are 1 963 and 213 m^3, respectively. Different splitters and combiners (**Jeppsson *et al.*, 2007**) are used to reproduce the effect of M and IC (the latter is kept at a constant value of 12 670 $m^3.day^{-1}$). At the *granular scale,* the number of granules (n_g)/total contact area (A_b) are calculated from VSS measurements (**Vangsgaard *et al.*, 2012),** and these values change as a function of reactor height. So does also the assumed maximum granule diameter ($L_{max,granule}$). Hence, in the lower reactor ($R1$) granules are assumed to heavier (due to gravity), bigger ($L_{max,granule,1}$) and more numerous ($n_{g,1}$). On the other hand, in the top reactor ($R2$) there is a lower number of granules ($n_{g,2}$) and they are smaller in size ($L_{max,granule,2}$) i.e. there is a vertical VSS gradient. No $L_{max,granule}$ measurement data was available and literature data was used **(Batstone et al., 2004**). In this way, the model describes a differential granular size distribution as a function of $R1$ and $R2$. For simplicity purposes, granules are assumed to be spherical and have constant density ($\rho_{biofilm}$ = 180 kg

COD.m^{-3}) (**Batstone *et al.*, 2004**). Finally, at the *biofilm scale*, a one-dimensional model is constructed according to **Wanner *et al.* (2006)**. The model contains both soluble (S) and particulate (X) state variables. The mass balance assumes that the transport of soluble compounds is governed solely by (homogenous) diffusion whereas movement of particulate compounds takes place by convection (**Saravanan and Sreekrishnan, 2006**) (see **Figure 1** for details). Biofilm thickness (L) is given as the radial distance (z) from the centre to the surface of the granule and varies due to two phenomena: the net growth of the particulate species and detachment from the biofilm surface (**Lackner *et al.*, 2008**). The resulting system of partial differential equations ($PDEs$) is solved using the method of lines (**Press *et al.*, 2007**). In this case, discretization of space (z = the radial distance) is chosen to obtain a system of ordinary differential equations ($ODEs$). The second order space derivative describing diffusion (S only) is approximated by the finite central difference method in spherical coordinates. The first order derivative for convective movement of X is solved using a backward difference approximation of the first order concentration space derivative (unless it is the first node, where it is a forward difference). The integral in the equation describing the biofilm growth velocity is approximated by the trapezoidal rule. Further information about biofilm/bulk mass balancing, boundary conditions and numerical resolution can be found in **Vangsgaard *et al.* (2012)**. The model has been implemented from these first principles in Matlab-Simulink (Mathworks, Natick, MA, USA). All dynamic simulations are preceded by steady state simulations to ensure correct model initialization (**Gernaey *et al.*, 2014**). Constant influent conditions for each $\#D1$, $\#D2$ are calculated using average influent values and thus avoiding deviations in the granule composition. Additional details regarding model assumption, model parameters and simulation procedure can be found in the Supplemental Information (**Table S7**).

2.6. Parameter estimation

Optimum values of kinetic coefficients for selected model parameters were estimated by separately fitting results to the dataset from each campaign ($\#D1$, $\#D2$), using a non-linear local optimization technique, lsqcurvefit, in MATLAB with the default 'trust-region-reflective' algorithm (**Mathworks, Natick, MA, USA**). The residual sum of squares (RSS) was used as objective function. Further information about the method can be found elsewhere (**Lobry *et al.*, 1991**). Key parameters affecting biogas (CH_4, CO_2, H_2S), organics profiles (COD_{part}, COD_{sol}, VFA), nutrients (NH_{x}, $H_{\mathrm{x}}PO_4^{3-\mathrm{x}}$) and several cations/anions (SO_{x}^{2-},

Ca^{2+}, Mg^{2+}) are estimated. The selection of these parameters is based on previous global sensitivity analysis studies (**Solon *et al.*, 2015b; Barrera *et al.*, 2015**).

3. MODEL PREDICTION CAPABILITIES

3.1. Dynamic modelling of influent data

Figure 2 illustrates that the $BSM2$ influent generator is able to reproduce flow-rate and pollution ($VFAs$, COD, N, P & S) trends for the two studied data sets ($\#D1$ and $\#D2$) Simulation results demonstrate that the assumed specific user-defined profiles can produce influent data with high frequency. The generated plots show some additional daily (day 15 $\#D1$ and day 13 $\#D2$) and weekly variations (day 7 in $\#D1$ & day 8 $\#D2$), the effect of cleaning equipment within the production site (day 15 in $\#D1$) and shutting down the reactor (day 4 and 11 in $\#D2$), which was not originally available for all the influent measurements. **Table S0** show that the average deviation for both $\#D1, \#D2$ is around 5 %. The influent files created by the $BSM2$ influent generator will then be fed to the multi-scale reactor model for subsequent testing.

3.2. Dynamic modelling of effluent data

Simulation results (solid lines) show that the proposed approach is capable of reproducing (dotted lines) hydrolysis (see COD_{part} profiles), acidogenesis (see COD_{sol} profiles) and acetogenesis (see VFA profiles) for $\#D1$ (see **Figure 3**). The pH, SO_x^{2-}, CH_4, CO_2 and H_2S profiles reveal the correct description of the weak acid-base chemistry, mass transfer (liquid-gas) methanogenesis, sulfidogenesis and competition between methanogens (MET) and sulfate reducing bacteria (SRB). The model also predicts N (see NH_x profiles) and P (see $H_xPO_4^{3-x}$ profiles) release with good agreement. Finally, although the SI values identify potential precipitation of $CaCO_3$ and $Ca_3(PO_4)_2$, the mass balances indicate that this does not occur (or if it does to a very low degree) (see Ca^{2+} and Mg^{2+} profiles). Average deviation between measurements and simulations for $\#D1$ is 10.2 % (see **Table S9**)

Influent characterization is based on rigorous COD, N, P & S mass balances, and follows the principles reported in **Feldman *et al.* (2017)** (see **Tables S1, S2, S3, S4** and **S5** in the supplemental information section). Kinetic parameters were estimated as described in Section 2.6. Compared to the default values (considering not X_c as stated in **Bastone *et al.*, 2015**), hydrolysis rates (k_{carb}, k_{prot}, k_{lip}) had to be increased

considerably (around 10 times). This is mainly due to extremely biodegradable influent (around 70 % of the total COD is converted to CH_4). The $preAD$ tank before the AD does contribute to that purpose as the degree of acidification (DA) in the influent and effluent is 40 %. Another potential reason could be the over-estimation of the influent X_{I}. Moreover, uptake rates for hydrogen degraders ($X_{\mathrm{H_2}}, X_{\mathrm{SRB}}$) had to be slightly adjusted in order to give a competitive advantage to SRB (**Batstone *et al.*, 2006; Barrera *et al.*, 2015; Flores-Alsina *et al.*, 2016).** This study assumes that S conversion (around 50 % of the incoming S) is done autolithotrophically (**Batstone *et al.*, 2006; Flores-Alsina *et al.*, 2016**). The inhibition parameter for H_2S had to be decreased substantially ($K_{\mathrm{I,H2S}}$) in order to describe VFA dynamics effectively. The most probable reason is the potential inhibition on acetogens (X_{c4}, X_{pro} and X_{ac}) by an inorganic/organic/metal compound that is neither measured nor described by the model (**Chen *et al.*, 2008**). The N and P contents in biomass/inerts had to be re-estimated to match the nutrient dynamics. The other parameters were set to their default values (**Batstone *et al.*, 2002; Flores-Alsina *et al.*, 2016**). Further information about parameter values, as well as the deviation from default values, can be found in **Table S6** and **Table S7** in the Supplemental Information section.

Figure 4 shows the dynamic profiles for the second evaluation period ($\#D2$). The same procedure is used for influent and parameter characterization. Again, simulation results reveal that the model successfully predicts the trends of selected operational variables. The good agreement between the measured (dotted lines) and the simulated (solid lines) data supported that the developed multi-reactor scale model properly captures the interactions between the influent wastewater and relevant microorganisms (see in **Table S9** that average deviation measurement/simulation for $\#D2$ is 10.1 %). As the reader may notice, there were problems with the pH sensor during $\#D2$ and only occasional measurements were available (average values around 7.3). Another important difference with respect to $\#D1$ is the role of precipitation. The higher operational pH and Ca^{2+} and lower $H_{\mathrm{x}}PO_4^{3-\mathrm{x}}$ concentrations indicate that $CaCO_3$ is the dominant compound. High SI values and literature data (**Van Langerak *et al.*, 1998)** reinforce the hypothesis. The same rationale was used to select and adjust model parameters.

The same procedure is used to characterize influent fractions and select and estimate relevant parameters (see **Table S1-S5** in the Supplemental Information section). Specifically for $\#D2$, hydrolysis rate values

(k_{carb}, k_{prot}, k_{lip}) are closer to the values reported in **Batstone *et al.* (2015)**. This is attributed to the lower biodegradability of the substrate. Mass balances in **Table S1** show a decrease of the COD conversion to CH_4 from 70 to 60 % when comparing $\#D1$ with $\#D2$. The COD_{part} / COD_t ratio is also substantially higher (from 15 to 28 %) for $\#D2$. A higher S content in organics ($S_{proteins}$) and consequently in biomass ($S_{biomass}$) had to be applied to close the mass balances (see Supplemental Information section **Table S4**). Uptake rates for hydrogen degraders (X_{H_2}, X_{SRB}) are slightly modified. Despite the higher S load, a similar reduction (50 %) to sulfides is achieved (see **Table S5** in the Supplemental Information section). The value of the inhibition parameter for H_2S ($K_{I,H2S}$) is set back to the default values, which reenforce the previous hypothesis of the presence of an unidentified inhibiting compound for $\#D1$ (the DA in the effluent is lower). With respect to the precipitation kinetics, k_{CaCO_3} is close to the values reported by **Kazadi Mbamba *et al.* (2015b).** It is important to highlight that this study only considers precipitation in the bulk. The effect of inter-granular precipitation is studied in the following section. As in the previous case**,** the other parameters are set to their default values (**Batstone *et al.*, 2002; Flores-Alsina *et al.*, 2016**).

4. ADDITIONAL MODEL PREDICTIONS

The additional simulations presented in this section demonstrate some of the potential of using the proposed approach when performing model-based studies. Therefore, for exemplary purposes, the adjusted model will be used to: 1) analyse different multi-scale elements; and, 2) explore how results (using $\#D1$ and $\#D2$ and calibrated parameters) are affected by changing some of the model settings (steady state+dynamic). *Simulation 1* predicts the assumed distribution of key microorganisms from the core to the surface of the anaerobic granular sludge for $\#D1$ (in both $R1$ and $R2$). In *Simulation 2*, the impacts of operational pH and $S:COD$ ratio on: 1) biomass distribution; and, 2) methane production are studied for $\#D1$. Finally, *Simulation 3* shows the potential effect that intra-granular precipitation might have on the organic/inorganic ratio within the granule using $\#D2$ as a case study (where $CaCO_3$ formation takes place).

4.1. Relative substrate/biomass distribution within the granule

The simulation results depicted in **Figure 5** show the concentration profiles of fermentables (S_{su}, S_{aa}, S_{fa}, S_{EtOH}), organic acids (S_{va}, S_{bu}, S_{pro}, S_{ac}) and hydrogen (S_{H_2}) as a function of granule depth for both $R1$

($L_{\mathrm{max,granule,1}}$) and $R2$ ($L_{\mathrm{max,granule,2}}$). These substrates were predicted to degrade to a concentration level of approximately 10 % of the affinity constant K_{S} (**Batstone *et al.*, 2002**) within the outer 100 μm of the biofilm. Methane ($S_{\mathrm{CH_4}}$) and pH, on the other hand, show the opposite behaviour: higher values in the centre of the granule and a significant decrease towards the surface. Regarding $R1$ and $R2$ one can observe the same trends, but organic soluble substrates (S) and pH are higher in the lower reactor due to the higher loading conditions. The model also indicates that the centre of the granule is inactive due to the high concentration of inert material (X_{I}) resulting from biomass death. The biomass (X_{bio}) and organics (X_{org}) concentrations increase for an increasing radial distance (z), i.e. the closer to the surface, the higher the biomass concentration. Similar experimental observations were reported by **de Beer e*t al.* (1992), Flora *et al.* (1995), Batstone *et al.* (2004)** and **Saravanan and Sreekrishnan (2006).** Regarding the distribution of specific groups of microorganisms, a high portion of methanogens (X_{ac}) is placed in the inner zone, and this fraction decreases as the radius of the granule increases. The presence of acidogens ($X_{\mathrm{su}}, X_{\mathrm{aa}}, X_{\mathrm{fa}}$) and acetogens ($X_{\mathrm{c4}},\ X_{\mathrm{pro}}$) is comparatively higher in the outer layers of the biofilm (see **Figures 5** and **6,** first column), though it should be noted no clear demarcation zone in activity zones exists. The role of X_{SRB} is quite marginal due to limited turnover. This distribution responds to: 1) applied loading rates; 2) mass transfer limitations; 3) the specific (bacterial) affinity for substrates; and, 4) relative kinetic uptake rate of the substrates, as well as substrate placement within the overall process. Again, similar trends can be observed between the upper and lower reactors but there is a lower quantity of X_{I} in $R2$ due to loading conditions. Both uni/multi-dimensional models presented in **Batstone *et al.* (2004; 2006)** and **Odriozola *et al.* (2016)** have presented comparable predictions.

4.2. Impact of the operational/loading conditions

In the second scenario, the effects of a lower pH (decrease from 7 to 6) and higher S loads (3 times) are assessed. These scenarios are defined quite arbitrarily; it is just to show the reader how model predictions might change when the conditions (weak acid-base chemistry, $S{:}\,COD$) assumed in the previous section are modified. Simulation results reveal a decrease in the $G_{\mathrm{CH_4}}$values (by 15 and 30 %, respectively) as a result of lower concentrations of methanogenic bacteria. In the first case, this can be explained because $X_{\mathrm{H_2}}$ and X_{ac} have an optimal pH range between 6.5 and 7.5 (**Batstone *et al.*, 2002**). In the second case, the reduction is

attributed to: 1) sulfide inhibition of acetoclastic and hydrogenotrophic methanogenesis; and, 2) competition between SRB (X_{SRB}) and hydrogenotrophic methanogens (X_{H_2}) for electron equivalents (S_{H_2}). The increased S load results in a higher allocation of influent COD to S_{H_2S} instead of S_{CH_4}(**Chen *et al.*, 2008**; **Hao *et al.*, 2016**). **Figure 6** shows the biomass distribution inside the granule for the default case (column 1), and the two generated scenarios (columns 2 and 3). No substantial variations in microbial distributions can be observed. There is only an increase of the relative space occupied by X_{SRB} in column 3 (high S) since these organisms now gain a competitive advantage with respect to other groups. Additional 2-D plots are displayed in the Supplemental Information section. These results indicate that the biomass is resistant to changes in loading conditions and hence turnover and response in biomass structure dampened by low decay rates (**Batstone *et al.*, 2004)**. I

4.3. Intra-granular precipitation

The last scenario assumes also intra-granular instead of only bulk precipitation for $\#D2$. The TSS model presented in **Ekama *et al.* (2006)** is used to describe the organic/inorganic distribution within the granule. Precipitation kinetics are also based on equations described in **Kazadi Mbamba *et al.* (2015)** using the parameters adjusted for the bulk (see **Table S7** in the Supplemental Information). Simulated results of the organic/inorganic distribution and SI values for: 1) both $R1$ and $R2$; and, 2) different time points are illustrated in **Figure 7**. At time 0, the entire granule is basically organic, with a small fraction of inorganic particulates linked to intracellular inorganic compounds (**Ekama and Wentzel, 2004**). As time proceeds and precipitation is allowed to occur, the fraction of inorganics increases resulting in X_{CaCO_3} formation (see column 2 in **Figure 7**). This causes a reduction of the biogas production since precipitates compete with biomass for space within the biofilm (precipitates occupy around 20 % of the space). The distribution of inorganic particulates within the granule corresponds well with the SI predictions. The presented model suggests that precipitates are first formed in the centre of the granule due to the increasing pH gradients (see **Figure 5**), and relatively flat anion and cation concentration profiles. Similar conclusions are reported in the experimental observations carried out by **Uemura and Harada (1995), Manas *et al.* (2012)** and **Winkler *et al.* (2013)**. Next, due to convective movement, these precipitates are transported to the surface (see **Figure 7,** column 3). Finally, one might notice the vertical gradient in the distribution of inorganics. In the bottom

reactor ($R1$), there is a high degree of precipitation due to the high concentration of calcium and carbonates. On the other hand, in the top reactor where most of the Ca has been consumed, the inorganic content in the granules is lower.

5. DISCUSSION

The results summarized in this study bring a substantial advance in the field of wastewater treatment modelling by introducing a multi-scale representation of the anaerobic digestion process. At the *reactor level* the model describes general hydrodynamics accounting for high ($R1$) and low ($R2$) loading conditions, gas-liquid ($G-L$) transfer as well as multiple instances of flow combining (M) and flow spitting ($R1$). At the *granule level*, size is a function of biomass growth and decay. The maximum diameter is assumed to change with reactor height. Finally at the *biofilm* level, species competition/inhibition for substrates/space is described following well-established biochemical/physico-chemical models, like the ADM1. While these approaches are applied piecemeal in the literature, this paper demonstrates the strength of an integrated approach, using a comprehensive data set ($\#D1$, $\#D2$). Development of such models, including their validation with full-scale data, is critical to enable future development of better operational strategies or optimization studies (**Jeppsson *et al.*, 2013**), with particular opportunity in industrial systems. In the following section, the authors discuss the suitability of the number of considered processes and some practical implications for the plant-wide modelling of resource recovery strategies.

5.1. Opportunities and limitations

The approach presented in this manuscript offers a moderately parsimonious, yet mechanistic representation of the digestion process under study given the high complexity of the problem. The reader should be aware that the system under investigation is an industrial plant and the composition of the feed together with the way to operate the reactor changes substantially according to yearly production schemes, in comparison with the relative predictability of domestic wastewaters (see also introduction when describing some of the challenges related to industrial wastewater treatment). As discussed in the manuscript, this could explain the changes in the influent biodegradability (k_{carb}, k_{prot}, k_{lip}) and the unusually low ($K_{\mathrm{I,H2S}}$) values, which forced the re-estimation of a few parameters when switching from $\#D1$ to $\#D2$. Yet, the study has shown

that the model provides very reasonable predictions with minimal parameter value modifications. Indeed, almost all parameters are kept at their default values (see **Table S7** in the Supplemental Information section).

Additional experimental results are necessary to validate the predicted profiles within the biofilm. In that sense micro-sensors are promising tools (**Garcia-Robledo *et al.*, 2016**). The same applies to the prediction of the microbial distribution in the granules, which is far more readily evaluated using molecular techniques. This type of research is currently being done using fluorescence in-situ hybridisation (**Batstone *et al.*, 2004; Winkler *et al.*, 2013**), but also extraction and bulk methods are used (**Lu *et al.*, 2012**). Molecular techniques will provide additional insights on how microorganisms are distributed within the granule, and if this distribution changes as a function of: 1) reactor height; 2) ash content (quantity of precipitation); and, 3) granular sizes. A proper assessment of the last factor has not been performed in this study, and literature data was used instead. However, all this information will help to construct better mechanistic models and increase the overall knowledge about anaerobic (industrial) biofilms.

Model upgrades could substantially improve the model prediction capabilities (**Table S9** indicates room for improvement in some of the accounted processes). The consideration of extra inhibiting/toxic compounds (**Rosen *et al.*, 2004**) terms could move $K_{\mathrm{I,H2S}}$ to default values. Better characterization interfaces (**Zaher *el al.*, 2009**) linked with the influent generator would better describe influent biodegradability. The latter could reduce the differences between hydrolysis rates (k_{carb}, k_{prot}, k_{lip}). There are numerous studies demonstrating that the effect of granular size and granular size distribution have a strong impact on process (**Volcke *et al.*, 2010; 2012, Sun et al., 2016**). Additional simulations are included in the Supplemental information section showing the impact substantial impact of granule size on: mass transfer, biomass distribution and weak acid base chemistry. (**Figure S1**). The latter is translated to biogas production (Table S10). In this study, only one granular size ($L_{\mathrm{max,granule1}}$ and $L_{\mathrm{max,granule2}}$).was assumed for each considered CSTRs ($R1$ and $R2$) and kinetic parameter adjusted accordingly. Nevertheless, some modifications in the source code would allow us to consider different granular types within the same CSTR. In this case, the equation used to quantify n_{g} from VSS should be re-arranged. As well, in the bulk mass balance equations (S, X) the contribution of the different types of granules and relative abundance (A_{b}) considered. A higher number of CSTRs would better describe the vertical TSS gradients. The latter, but, would increase the

computational demand and therefore simulation time an already heavy model. This can be critical in systems with a clear competition between MET and SRB (**Cassidy *et al.*, 2016**). Indeed, at high SO_4^{-2} and $Et-OH$, SRB utilizing different types of organics ($S_{va}, S_{bu}, S_{pro}, S_{ac,} S_{etOH}$) as electron sources should be considered. The latter might affect the biomass distribution within the granule (**Liu *et al.*, 2015 a,b**; **Sun et al., 2016**). In this line of thinking, sulfide might have a strong influence of precipitation (location, characteristics) (**Villa Gomez et al., 2011, 2012**). In this paper, the assumption that precipitation was only taking place in the bulk worked out because the evaluation period was rather short. When considering a longer evaluation period, intra-granular precipitation must be included since it has a major importance in industrial reactors (**Van Langerak *et al.* 1998; 2000**). It is also a request from the process managers running the plant that future model development should include this type of phenomena. A first attempt is presented in the scenario analysis section, and is showing reasonable results. Nevertheless, this approach should be improved further by also including other aspects, such as the implementation of a proper biofilm density model (**Jiang e*t al.*, 2008; Winkler *et al.*, 2013**) or the modification of the diffusion coefficients proportionally to the degree of precipitation (**Keenan *et al.*, 1993; El-Mamouni *et al.*, 1995**).

An important aspect to take into account is related to the representation of the biomass and substrates presented in **Figures 5** to **7**. Indeed, the reader should be aware that the inner position within the granule correspond to minor volume fractions, and the mass associated to this volume if a minor fraction of the total mass of the species. This is can be clearly represented in the Supplemental information section, where for exemplary purposes a 2-D representation of the granule structure is depicted for the first scenario analysis discussed in section 4.1 (**Figure S2**). Even though the inner material seems to have an important contribution, in terms of mass the picture change dramatically.

Finally, it should be noticed that no systematic procedure has been used for model calibration **(Brockmann *et al.*, 2008; 2013**). The results of the global sensitivity analyses by **Solon *et al.* (2015b)** and **Barrera *et al.* (2015)** serve as a good indication and provide a good way to start. The methods might not be applicable in other systems, but in this case, the number of parameters to be adjusted was rather small in order to produce reasonable values.

5.2. Model based optimization of reactor performance

The model implementation presented in this paper will allow the development of benchmarking procedures for optimizing resource recovery (e.g. biogas recovery) in an industrial context (**Copp, 2002; Gernaey *et al.*, 2014**). Implementation of special routines has been necessary, to allow the use of non-stiff solvers (**Flores-Alsina *et al.*, 2015**). As a consequence, it is now also possible to use sophisticated sensor and actuator models accounting for different step responses, delay and noise levels (**Rieger *et al.*, 2003; Rosen *et al.*, 2008**). This will allow to develop, test, implement and evaluate realistic control strategies. This is a clear advantage with respect to state of the art biofilm software (**Reichert *et al.*, 1994**) allowing a whole new set of possibilities. Control strategies such as the ones presented in **Steyer *et al.* (1999), Irizar *et al.*, 2015** and **Stromberg *et al*. (2013)** could be tested as well in (anaerobic) granular systems.

The model has the potential to evaluate more traditional process options, such as the financial benefits resulting from an improved biogas production balanced against the addition of selected chemicals (**Flores-Alsina *et al.*, 2016**), calcium control **(Van Langerak et al., 1997**), or the addition of substrates for co-digestion (**Arnell *et al.*, 2016**). Appropriate performance evaluation indices should be developed for that purpose (**Solon *et al.*, 2017**). For example, one can evaluate the financial benefits of increasing methane production in terms of how much more energy (electricity, heat) is produced and consequently sold (or re-used within the factory). Another interesting alternative is to determine appropriate reactor sludge wasting schemes to cope with excessive precipitation. The study demonstrated that the model can be used to estimate the ratio of organics/inorganics in the granules at different cationic loads. Such information could improve the day to day operation of the reactor. Finally, the model is used to evaluate effluent COD/N and thus ensure a good (downstream) nitrogen removal process. Indeed, the AD conversion should also guarantee a sufficient quantity of VFA to allow downstream denitrification to proceed (organic acids act as electron acceptors). Subsequent studies are currently undertaken to overcome these limitations of the AD system – in terms of N removal capacity – by implementation of an Anammox system following the AD system. Experimental work (lab scale, pilot scale) is carried out to adapt existing models (**Vangsgaard *et al.*, 2012**) to the analysed industrial site. In this way, a combined anaerobic digestion-autotrophic denitrification model is being developed in order to conduct fully integrated studies.

6. CONCLUSION

The main findings of the presented study can be summarized in the following points:

- A multi-scale mathematical model approach is developed and used to predict the performance of an industrial full-scale anaerobic digester. The model deals with reactor hydrodynamic issues, granule growth, gas stripping, intra-granular convective movement and mass transfer limitations as well as multi-species/multi-substrate competition/inhibition within the biofilm.
- The modified version of the BSM2 influent generator provided additional dynamics (diurnal & weekly variation/cleaning of equipment/ reactor shut down) and increased data frequency (from days to minutes).
- The model is capable to describe hydrolysis, acidogenesis, acetogenesis, methanogenesis, sulfidogenesis, liquid-gas mass transfer, weak acid-base chemistry and multiple mineral precipitation as demonstrated by the good agreement between the (macroscopic) experimental data and the model simulations (average deviation for both $\#D1$, $\#D2$ is around 10 %) .
- The potential biomass distribution within the granule and for each reactor is assessed based on influent loadings, mass transfer limitations and bacterial affinity for substrate. Competition between inorganics (precipitates) and organics (biomass) can be analyzed on the basis of the developed models.
- The set of models presented in this study can be used as an engineering tool to aid decision makers/wastewater engineers when upgrading/improving the sustainability and efficiency of wastewater treatment systems (e.g. avoid MET and SRB competition, reduce consumption of chemicals and increase energy recovery).

7. SOFTWARE AVAILABILITY

The Matlab-Simulink code of the model presented in this paper is available upon request, including the implementation of the physico-chemical (PCM) and biological (ADM1) modelling framework in granular sludge reactors (BIOFILM). Using this code, interested readers will be able to reproduce the results summarized in this study. To express interest, please contact Prof. Krist V. Gernaey (kvg@kt.dtu.dk) or Dr. Xavier Flores-Alsina (xfa@kt.dtu.dk) at the Technical University of Denmark (Denmark).

8. ACKNOWLEDGEMENTS

This work was done in collaboration with Novozymes A/S, Denmark. Financial support for the project from Novozymes A/S and the Technical University of Denmark is gratefully acknowledged. Dr Flores-Alsina gratefully acknowledges the financial support of the collaborative international consortium WATERJPI2015 WATINTECH of the Water Challenges for a Changing World Joint Programming Initiative (Water JPI) 2015 call. A concise version of this paper was presented at the IWA conferences on Biofilm Systems (Dublin, Ireland, May, 2017) and Instrumentation, Control and Automation (ICA) (Québec, Canada, June, 2017).

9. REFERENCES

APHA, 2012. Standard Methods for the Examination of Water and Wastewater. American Public Health Association, Washington, DC, USA.

Arnell M., Astals S., Åmand L., Batstone D.J., Jensen P.D. & Jeppsson U. (2016). Modelling anaerobic co-digestion in Benchmark Simulation Model No. 2: Parameter estimation, substrate characterisation and plant-wide integration. Water Research, 98, 138-146.

Astals S., Esteban-Gutiérrez M., Fernández-Arévalo T., Aymerich E., García-Heras J.L. & Mata-Alvarez J. (2013). Anaerobic digestion of seven different sewage sludges: A biodegradability and modelling study. Water Research, 47(16), 6033-6043.

Aymerich E., Esteban-Gutierrez M., Roche E., Suescun J., Irizar I. Practical experiences on simulating full-scale IC reactors for pulp and paper mill wastewater, 14th World Congress on Anaerobic Digestion, Viña del Mar, Chile, 15-18 November 2015.

Barrera E.L., Spanjers H., Solon K., Amerlinck Y., Nopens I. & Dewulf J. (2015). Modeling the anaerobic digestion of cane-molasses vinasse: Extension of the Anaerobic Digestion Model No. 1 (ADM1) with sulfate reduction for a very high strength and sulfate rich wastewater. Water Research, 71, 42-54.

Batstone D.J. (2006). Mathematical modelling of anaerobic reactors treating domestic wastewater: Rational criteria for model use. Reviews in Environmental Science and Biotechnology, 5, 57-71.

Batstone D.J., Hernandez J.L.A. & Schmidt J.E. (2005). Hydraulics of laboratory and full-scale upflow anaerobic sludge blanket (UASB) reactors. Biotechnol. Bioeng., 91, 387-391.

512 Batstone D.J. & Keller J. (2003). Industrial application of the IWA Anaerobic Digestion Model No.1
513 (ADM1). Wat. Sci. Tech., 47(12), 199-206.

514 Batstone D.J., Keller J., Angelidaki I., Kalyuzhnyi S.V., Pavlostathis S.G., Rozzi A., Sanders W.T.M.,
515 Siegrist H. & Vavilin V.A. (2002). Anaerobic Digestion Model No. 1. IWA Scientific and Technical Report
516 No. 13. London, UK: IWA Publishing.

517 Batstone D.J., Keller J. & Blackall L.L. (2004b). The influence of substrate kinetics on the
518 microbialcommunity structure in granular anaerobic biomass. Water Research, 38(6), 1390-1404.

519 Batstone D.J., Puyol D., Flores-Alsina X. & Rodriguez J. (2015). Mathematical modelling of anaerobic
520 digestion processes: Applications and future needs. Reviews on Environmental Science and Biotechnology,
521 14(4), 595-613.

522 Batstone D.J., Torrijos M.J., Ruiz C. & Schmidt J.E. (2004a). Use of an anaerobic sequencing batch reactor
523 for parameter estimation in modelling of anaerobic digestion. Wat. Sci. Tech., 50(10), 295-303.

524 Benedetti L., De Keyser W., Nopens I. & Vanrolleghem P.A. (2010). Probabilistic modelling and evaluation
525 of waste water treatment plant upgrades in the EU Water Framework Directive context. J. Hydroinformatics,
526 12(4), 380-395.

527 Boltz J.P., Morgenroth E., Brockmann D., Bott C., Gellner W.J. & Vanrolleghem P.A. (2011). Systematic
528 evaluation of biofilm models for engineering practice: components and critical assumptions. Wat. Sci. Tech.,
529 64(4), 930-944.

530 Brockmann D., Caylet A., Escudié R., Steyer J.-P. & Bernet N. (2013). Biofilm model calibration and
531 microbial diversity study using Monte Carlo simulations. Biotechnol. Bioeng., 110(5), 1323-1332.

532 Brockmann D., Rosenwinkel K.H. & Morgenroth E. (2008). Practical identifiability of biokinetic parameters
533 of a model describing two-step nitrification in biofilms. Biotechnol. Bioeng., 101(3), 497-514.

534 Cassidy J, Lubberding H.J., Esposito G., Keesman K.J., Lens P.N.L. Automated biological sulphate
535 reduction: A review on mathematical models, monitoring and bioprocess control. FEMS Microbiology
536 Reviews 39, (6): 823-853

537 Chen Y., Cheng J.J. & Creamer K.S. (2008). Inhibition of anaerobic digestion process: A review. Bioresour.
538 Technol., 99, 4044-4064.

539 Chen Z., Hu D., Zhang Z., Ren N. & Zhu H. (2009). Modeling of two phase anaerobic process treating
540 traditional Chinese medicine wastewater with the IWA Anaerobic Digestion Model No. 1. Bioresour.
541 Technol., 100, 4623-4631.
542 Copp J.B. (ed.) (2002). The COST Simulation Benchmark: Description and Simulator Manual. ISBN 92-
543 894-1658-0, Office for Official Publications of the European Community, Luxembourg.
544 Daigger G.T. (2011). Changing paradigms: From wastewater treatment to resource recovery. Proceedings of
545 the Water Environment Federation, 2011(6), 942-957.
546 De Beer D., Huisman J.W., van den Heuvel J.C. & Ottengraf S.P.P. (1992). The effect of pH profiles in
547 methanogenic aggregates on the kinetics of acetate conversion. Water Research, 26(10), 1329-1336.
548 de Gracia M., Sancho L., García-Heras J.L., Vanrolleghem P. & Ayesa E. (2006). Mass and charge
549 conservation check in dynamic models: Application to the new ADM1 model. Wat. Sci. Tech., 53(1), 225-
550 240.
551 Dereli R.K., Ersahin M.E., Ozgun H., Ozturk I. & Aydin A.F. (2010). Applicability of Anaerobic Digestion
552 Model No.1 (ADM1) for a specific industrial wastewater: Opium alkaloid effluents. Chem. Eng. J., 165(1),
553 89-94.
554 Ekama G.A. & Wentzel M.C. (2004). A predictive model for the reactor inorganic suspended solids
555 concentration in activated sludge systems. Water Research, 38(8), 4093-4106.
556 Ekama G.A., Wentzel M.C. & Sötemann S.W. (2006). Tracking the inorganic suspended solids through
557 biological treatment units of wastewater treatment plants. Water Research, 40(19), 3587-3595.
558 EI-Mamouni R., Guiot S.R., Mercier P., Sail B. & Samson R. (1995). Liming impact on granules activity of
559 the multiplate anaerobic reactor (MPAR) treating whey permeate. Bioprocess Engineering, 12, 47-53.
560 Ersahin M.E., Dereli R.K., Insel G., Ozturk I. & Kinaci C. (2007). Model based evaluation for the anaerobic
561 treatment of corn processing wastewaters. Clean-Soil Air Water, 35(6), 576-581.
562 Fang H.H. & Liu H. (2002). Effect of pH on hydrogen production from glucose by a mixed culture.
563 Bioresour. Technol., 82, 87-93.
564 Fedorovich V., Lens P. & Kalyuzhnyi S. (2003). Extension of Anaerobic Digestion Model No. 1 with
565 processes of sulfate reduction. Applied Biochemistry and Biotechnology, 109, 33-45.

Feldman H., Flores-Alsina X., Ramin P., Kjellberg K., Jeppsson U., Batstone D.J., Gernaey K.V. (2017). Model based optimization of a full-scale industrial high rate anaerobic bioreactor. Submitted to Biotechnology and Bioengineering.

Flora J.R.V., Suidan M.T., Biswas P. & Sayles G.D. (1995). A modelling study of anaerobic biofilm systems: I. Detailed biofilm modelling. Biotechnol. Bioengng. 46, 43-53.

Flores-Alsina X., Corominas L., Neumann M.B. & Vanrolleghem P.A. (2012). Assessing the use of activated sludge processs design guidelines in wastewater treatment plant projects. Env. Mod. Softw., 38, 50-58.

Flores-Alsina X., Kazadi Mbamba C., Solon K., Vrecko D., Tait S., Batstone D.J., Jeppsson U. & Gernaey K.V. (2015). A plant-wide aqueous phase chemistry module describing pH variations and ion speciation/pairing in wastewater treatment models. Water Research, 85, 255-265.

Flores-Alsina X., Saagi R., Lindblom E., Thirsing C., Thornberg D., Gernaey K.V. & Jeppsson U. (2014). Calibration and validation of a phenomenological influent pollutant disturbance scenario generator using full-scale data. Water Research, 51, 172-185.

Flores-Alsina X., Solon K., Kazadi Mbamba C., Tait S., Jeppsson U., Gernaey K.V. & Batstone D.J. (2016). Modelling phosphorus, sulphur and iron interactions during the dynamic simulation of anaerobic digestion processes. Water Research, 95, 370-382.

Garcia-Robledo E., Ottosen L.D.M., Voigt N.V., Kofoed M.W. & Revsbech N.P. (2016). Micro-scale H_2–CO_2 dynamics in a hydrogenotrophic methanogenic membrane reactor. Front. Microbiol., 17 (7)1276.

Gernaey K.V., Flores-Alsina X., Rosen C., Benedetti L. & Jeppsson U. (2011). Dynamic influent pollutant disturbance scenario generation using a phenomenological modelling approach. Environmental Modelling & Software, 26(11), 1255-1267.

Gernaey K.V., Jeppsson U., Vanrolleghem P.A. & Copp J.B. (2014). Benchmarking of control strategies for wastewater treatment plants. IWA Scientific and Technical Report No. 23. London, UK: IWA Publishing.

Hao T.W., Xiang P.Y., Mackey H.R., Chi K., Lu H., Chui H.K., van Loosdrecht M.C.M & Chen G.H. (2014). A review of biological sulfate conversions in wastewater treatment. Water Research, 65, 1-21.

Henze M., Gujer W., Mino T. & van Loosdrecht M.C.M. (2000). Activated Sludge Models ASM1, ASM2, ASM2d, and ASM3. IWA Scientific and Technical Report No. 9. London, UK: IWA Publishing.

Henze M., van Loosdrecht M.C.M., Ekama G.A. & Brdjanovic D. (2008). Biological wastewater treatment. London, UK: IWA Publishing.

Hinken L., Huber M., Weichgrebe D. & Rosenwinkel K.H. (2014). Modified ADM1 for modelling an UASB reactor laboratory plant treating starch wastewater and synthetic substrate load tests. Water Research, 64, 82-93.

Hug T., Benedetti L., Hall E.R., Johnson B.R., Morgenroth E., Nopens I., Rieger L., Shaw A. & Vanrolleghem P.A. (2009). Wastewater treatment models in teaching and training: The mismatch between education and requirements for jobs. Wat. Sci. Tech., 59(4), 745-753.

Irizar I., Zambrano J, Carlsson B., Morrás M., Aymerich E (2015). Robust tuning of bending-points detection algorithms in batch-operated processes: Application to Autothermal Thermophilic Aerobic Digesters", Environmental Modelling & Software, 71,148-158.

Jeppsson U., Alex J., Batstone D., Benedetti L., Comas J., Copp J.B., Corominas L., Flores-Alsina X., Gernaey K.V., Nopens I., Pons M.-N., Rodriguez-Roda I., Rosen C., Steyer J.-P., Vanrolleghem P.A., Volcke E.I.P. & Vrecko D. (2013). Benchmark simulation models, quo vadis?. Wat. Sci. Tech., 68(1), 1-15.

Jeppsson U., Pons M.N., Nopens I., Alex J., Copp J.B., Gernaey K.V., Rosen C., Steyer J.P. & Vanrolleghem P.A. (2007). Benchmark Simulation Model No 2 – General protocol and exploratory case studies. Wat. Sci. Tech., 56(8), 287-295.

Jiang F., Leung D.H., Li S., Chen G.H., Okabe S. & van Loosdrecht M.C.M. (2009). A biofilm model for prediction of pollutant transformation in sewers. Water Research, 43(13), 3187-3198.

Kalyuzhnyi S.V. & Fedorovich V.V. (1998). Mathematical modelling of competition between sulphate reduction and methanogenesis in anaerobic reactors. Bioresource Technology, 65, 227-242.

Kazadi Mbamba C., Flores-Alsina X., Batstone D.J. & Tait S. (2015a). A generalised chemical precipitation modelling approach in wastewater treatment applied to calcite. Water Research, 68, 342-353.

Kazadi Mbamaba C., Flores-Alsina X., Batstone D.J. & Tait S. (2015b). A systematic study of multiple minerals precipitation modelling in wastewater treatment. Water Research, 85, 359-370.

Keenan P.J., Isa J. & Switzenbaum M.S. (1993). Inorganic solids development in a pilot-scale anaerobic reactor treating municipal solid waste landfill leachate. Water. Environ. Res., 65, 181-188.

Lackner S., Terada A. & Smets B.F. (2008). Heterotrophic activity compromises autotrophic nitrogen removal in membrane-aerated biofilms: Results of a modeling study. Water Research, 42(4-5), 1102-1112.

Liu, Y, Zhang, Y & Ni, B.J. (2015a). Evaluating enhanced sulfate reduction and optimized volatile fatty acids (VFA) composition in anaerobic reactor by Fe (III) addition. Environmental Science and Technology, 49(4), 2123-2321.

Liu, Y, Zhang, Y & Ni B.J. (2015b). Zero valent iron simultaneously enhances methane production and sulfate reduction in anaerobic granular sludge reactors. Water Research, 75, 292-300.

Lobry J., Rosso L. & Flandrois, J. (1991). A FORTRAN subroutine for the determination of parameter confidence limits in non-linear models. Binary, 3, 86-93.

Lu Y., Slater F.R., Bello-Mendoza R. & Batstone D.J. (2012). Shearing of biofilms enables selective layer based microbial sampling and analysis. Biotechnology and Bioengineering, 110(10), 2500-2605.

Mañas A., Biscansa B. & Spérandio M. (2011). Biologically induced phosphorus precipitation in aerobic granular sludge process. Water Research, 45(12), 3776-3786.

Odriozola M., Lopez I. & Borzacconi L. (2016). Modelling granule development and reactor performance on anaerobic granular sludge reactors. Journal of Environmental and Chemical Engineering, 4, 1615-1628.

Press H., Teukolsky S.A., Vetterling W.T. & Flannery B.P. (2007). Numerical recipes: The art of scientific computing (3rd ed.). New York, NY, USA: Cambridge University Press.

Punal A, Trevisan M, Rozzi A & Lema L. (2000). Influence of C:N ratio on the start-up of up-flow anaerobic filter reactors. Water Research, 34(9), 2614-2619.

Reichert P. (1994). AQUASIM – a tool for simulation and data analysis of aquatic systems. Wat. Sci. Tech., 30(2), 21-30.

Rieger L., Alex J., Winkler S., Boehler M., Thomann M. & Siegrist H. (2003). Progress in sensor technology – Progress in process control. Part I: Sensor property investigation and classification. Wat. Sci. Tech., 47(2), 103-112.

Rittmann B.E. & McCarty P.L. (1980). Model of steady-state-biofilm kinetics. Biotechnol. Bioeng., 22(11), 2343-2357.

Rivas A., Irizar I. & Ayesa E. (2008). Model-based optimisation of wastewater treatment plants design. Environ. Modell. Softw., 23(4), 435-450.

Rodriguez-Roda I., Sànchez-Marrè M., Comas J., Baeza J., Colprim J., Lafuente J., Cortes U. & Poch M. (2002). A hybrid supervisory system to support WWTP operation: Implementation and validation. Wat. Sci. Tech., 45(4-5), 289-297.

Rosen C., Jeppsson U. & Vanrolleghem P.A. (2004). Towards a common benchmark for long-term process control and monitoring performance evaluation. Water Sci. Technol., 50(11), 41-49.

Rosen C., Jeppsson U., Rieger L. & Vanrolleghem P.A. (2008). Adding realism to simulated sensors and actuators. Wat. Sci. Tech. 57(3), 337-344.

Saravanan V. & Sreekrishnan (2006). Modelling anaerobic biofilm reactors – A review. Journal of Environmenal Management, 81, 1-18.

Snip L.J.P., Flores-Alsina X., Aymerich I., Rodríguez-Mozaz S., Barceló D., Plósz B.G., Corominas L., Rodriguez-Roda I., Jeppsson U. & Gernaey K.V. (2016). Generation of synthetic data to perform (micro) pollutant wastewater treatment modelling studies. Science of the Total Environment, 569-570, 278-290.

Solon K., Flores-Alsina X., Gernaey K.V. & Jeppsson U. (2015b). Effects of influent fractionation, kinetics & stoichiometry and mass transfer on CH_4, H_2 and CO_2 production for (plant-wide) modelling of anaerobic digesters. Wat. Sci. Tech., 71(6), 870-877.

Solon K., Flores-Alsina X., Kazadi-Mbamba C., Ikumi D., Volcke E.I.P, Vaneeckhaute C., Ekama G., Vanrolleghem P.A, Batstone D.J., Gernaey K.V. & Jeppsson U. (2017). Plant-wide modelling of phosphorus transformations in wastewater treatment systems: Impacts of control and operational strategies. Water Research, 113, 97-110.

Solon K., Flores-Alsina X., Kazadi Mbamba C., Volcke E.I.P., Tait S., Batstone D.J., Gernaey K.V. & Jeppsson U. (2015a). Effects of ionic strength and ion pairing on (plant-wide) modelling of anaerobic digestion processes. Water Research, 70, 235-245.

Steyer J.P., Buffière P., Rolland D. & Moletta R. (1999). Advanced control of anaerobic digestion processes through disturbance monitoring. Water Research, 33(9), 2059-2068.

Strömberg S., Possfelt M.O. & Liu J. (2013). Computer simulation of control strategies for optimal anaerobic digestion. Wat. Sci. Tech., 67(3), 594-603.

675 Sun J., Dai X., Wang Q., Pan Y. & Ni B.J. (2016). Modelling methane production and sulfate reduction in
676 anaerobic granular sludge reactor with ethanol as electron donor. Nature, Scientific reports 6, Article
677 number: 3531.
678 Tchobanoglous G., Burton F.L. & Stensel H.D. (2003). Wastewater Engineering: Treatment and Reuse (4th
679 ed.). New York, , New York, USA: McGraw-Hill Education.
680 Uemura S. & Harada H. (1995). Inorganic composition and microbial characteristics of methanogenic
681 granular sludge grown in a thermophilic upflow anaerobic sludge blanket reactor. Appl. Microbiol.
682 Biotechnol., 43(2), 358-364.
683 van Langerak E.P.A., Hamelers H.V.M., Lettinga G. (1997). Influent calcium removal by crystallization
684 reusing anaerobic effluent alkalinity. Wat. Sci. Tech., 36(6-7), 341-348.
685 van Langerak E.P.A., Gonzalez-Gil G., van Aelst A., van Lier J.B., Hamelers H.V.M. & Lettinga G. (1998).
686 Effects of high calcium concentrations on the development of methanogenic sludge in upflow anaerobic
687 sludge bed (UASB) reactors. Water Research, 32(4), 1255-1263.
688 Van Langerak E.P.A., Ramaekers H., Weichers A.H.M., Veeken H.V, Hamelers H.V.M. & Lettinga G.
689 (2000). Impact of location of $CaCO_3$ precipitation on development of intact anaerobic sludge. Water
690 Research, 34(2), 437-446.
691 Van Lier J. (2015). Celebrating 40 years anaerobic sludge bed reactors for industrial wastewater treatment.
692 Reviews in Environmental Science and Bio/Technology, 14(14), 681-702.
693 Vangsgaard A.K., Mauricio-Iglesias M., Gernaey K.V., Smets B.F. & Sin G. (2012). Sensitivity analysis of
694 autotrophic N removal by a granule based bioreactor: Influence of mass transfer versus microbial kinetics.
695 Bioresource Technol., 123, 230-241.
696 Villa-Gomez D. K., Ababneh H., Papirio S., Rousseau D.P.L., Lens, P.N.L., 2011. Effect of sulfide
697 concentration on the location of the metal precipitates in inversed fluidized bed reactors. Journal of
698 Hazardous Materials 192, 200-207.
699 Villa-Gomez D. K., Papirio S., van Hullebusch E.D., Farges F., Nikitenko S., Kramer H. and Lens P.N.L.
700 (2012). Influence of sulfide concentration and macronutrients on the characteristics of metal precipitates
701 relevant to metal recovery in bioreactors. Bioresource Technology 110 (0):26-34

Volcke E.I.P., Picioreanu C., De Baets B. & van Loosdrecht M.C.M. (2010). Effect of granule size on autotrophic nitrogen removal in a granular sludge reactor. Environ. Technol., 31(11), 1271-1280.

Volcke E.I.P., Picioreanu C., De Baets B. & van Loosdrecht M.C.M. (2012). The granule size distribution in an Anammox-based granular sludge reactor affects the conversion – Implications for modeling. Biotechnol. Bioeng., 109(7), 1629-1636.

Wanner O., Eberl H.J., Morgenroth E., Noguera D.R., Picioreanu C., Rittmann B.E. & van Loosdrecht M.C.M. (2006). Mathematical modeling of biofilms. IWA Scientific and Technical Report No. 18. London, UK: IWA Publishing.

Winkler M.K, Kleerebezem R., Strous M., Chandran K. & van Loosdrecht M.C.M. (2013). Factors influencing the density of aerobic granular sludge. Appl. Microbiol. Biotechnol., 97(16), 7459-7468.

Xavier J.B., Picioreanu C. & van Loosdrecht M.C.M. (2005). A framework for multidimensional modelling of activity and structure of multispecies biofilms. Environ. Microbiol., 7, 1085-1103.

Xu X-J, Chen C., Wang A.J., Ni B.J., Guo W.K, Yuan Y, Huang C.,Zhou X., Wu D.H, Lee D.H., Ren W.Q. (2017). Mathematical modeling of simultaneous carbon-nitrogen-sulfur removal from industrial wastewater. Journal of Hazardous Materials. 321, 371-381

Zaher, U., Rongping, L., Jeppsson, U., Steyer, J.-P., Chen, S., 2009. GISCOD: general integrated solid waste co-digestion model. Water Res. 43 (10), 2717-2727.

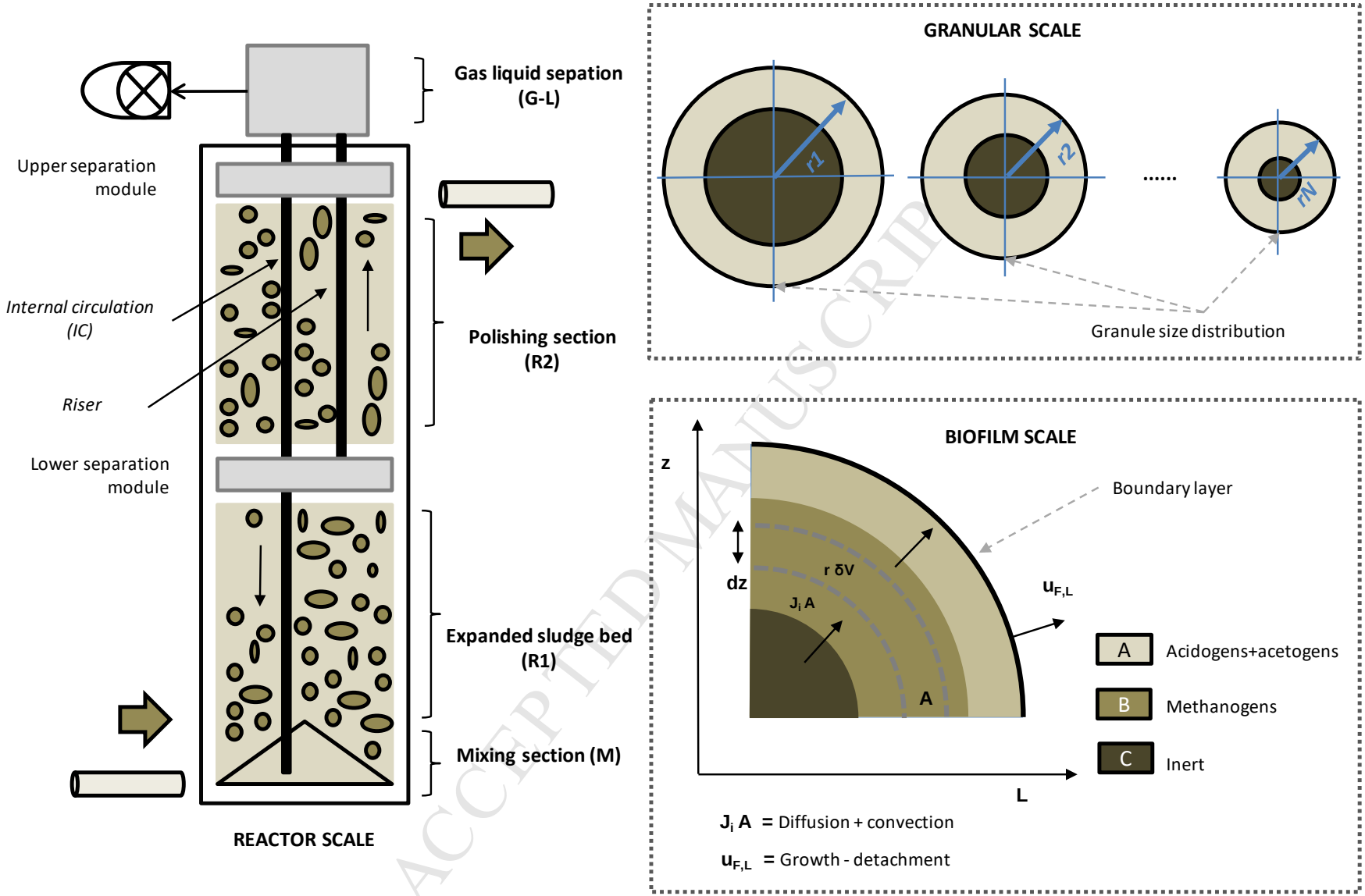

Figure 1. Multi-scale (reactor/biofilm/granule) representation of the proposed model.

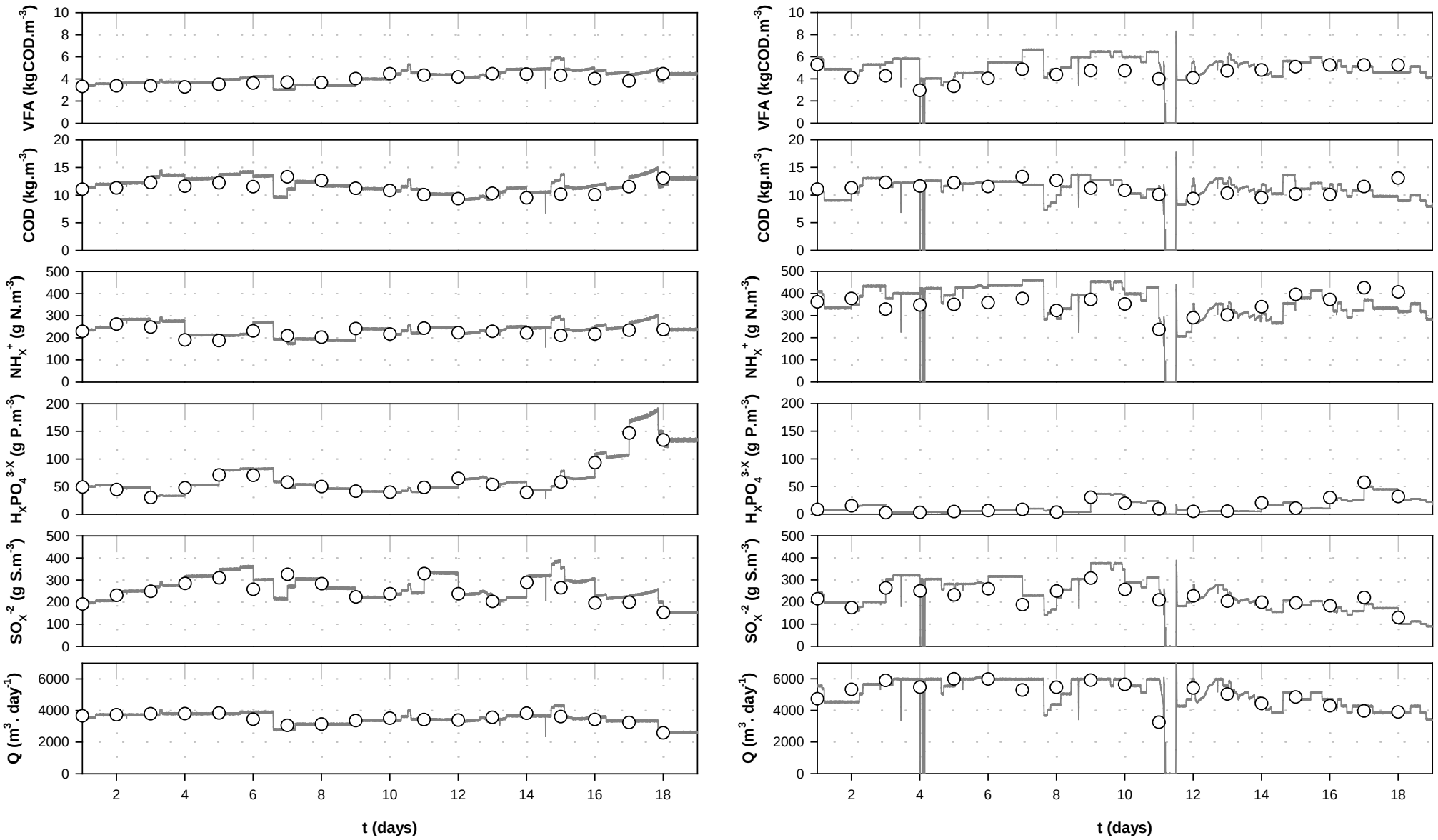

Figure 2. Simulation results and measured influent data for data set 1 (#*D*1) (left column) and 2 (#*D*2) (right column).

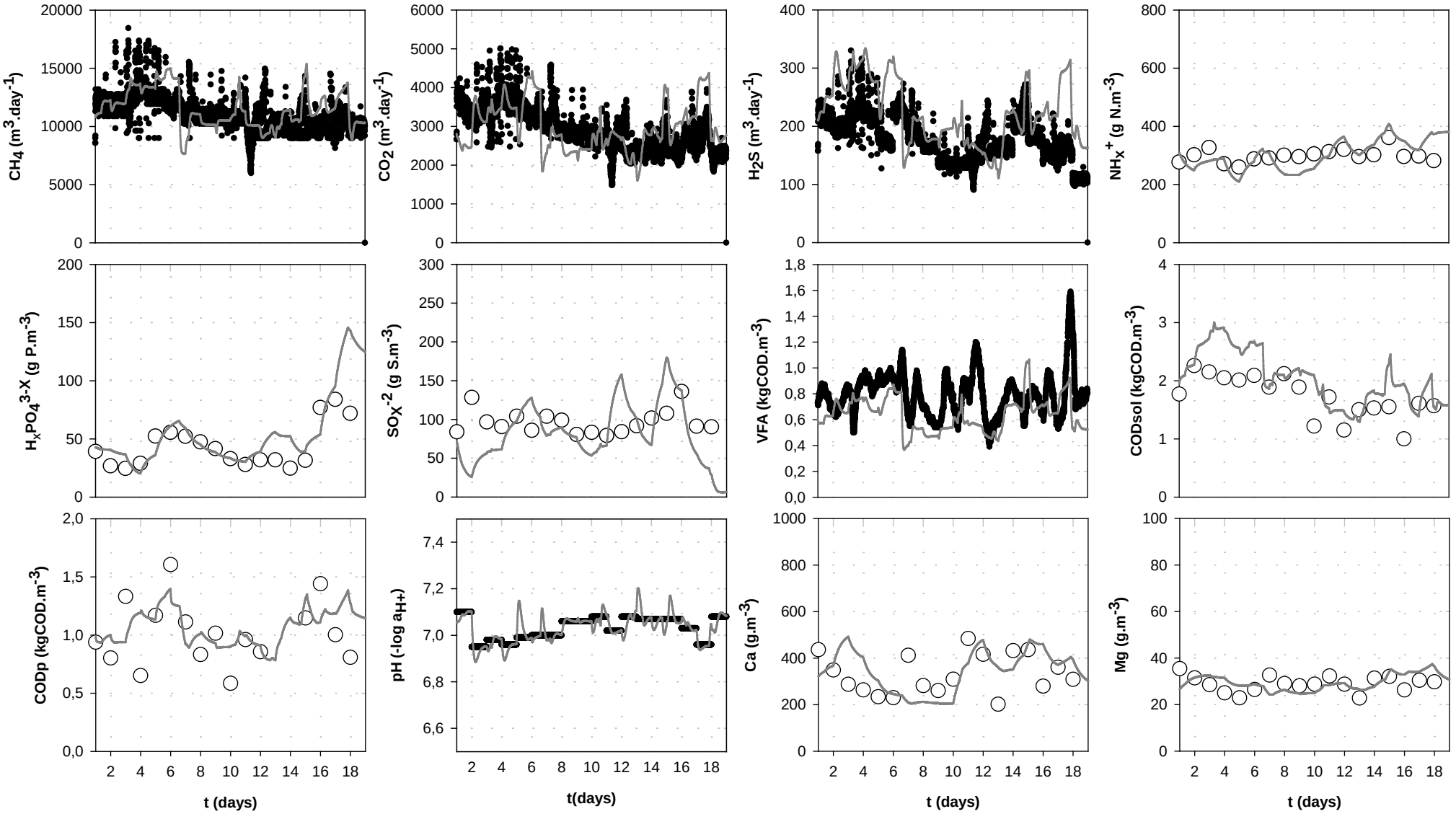

Figure 3. Simulation results and measured effluent data for data set 1 (#*D*1).

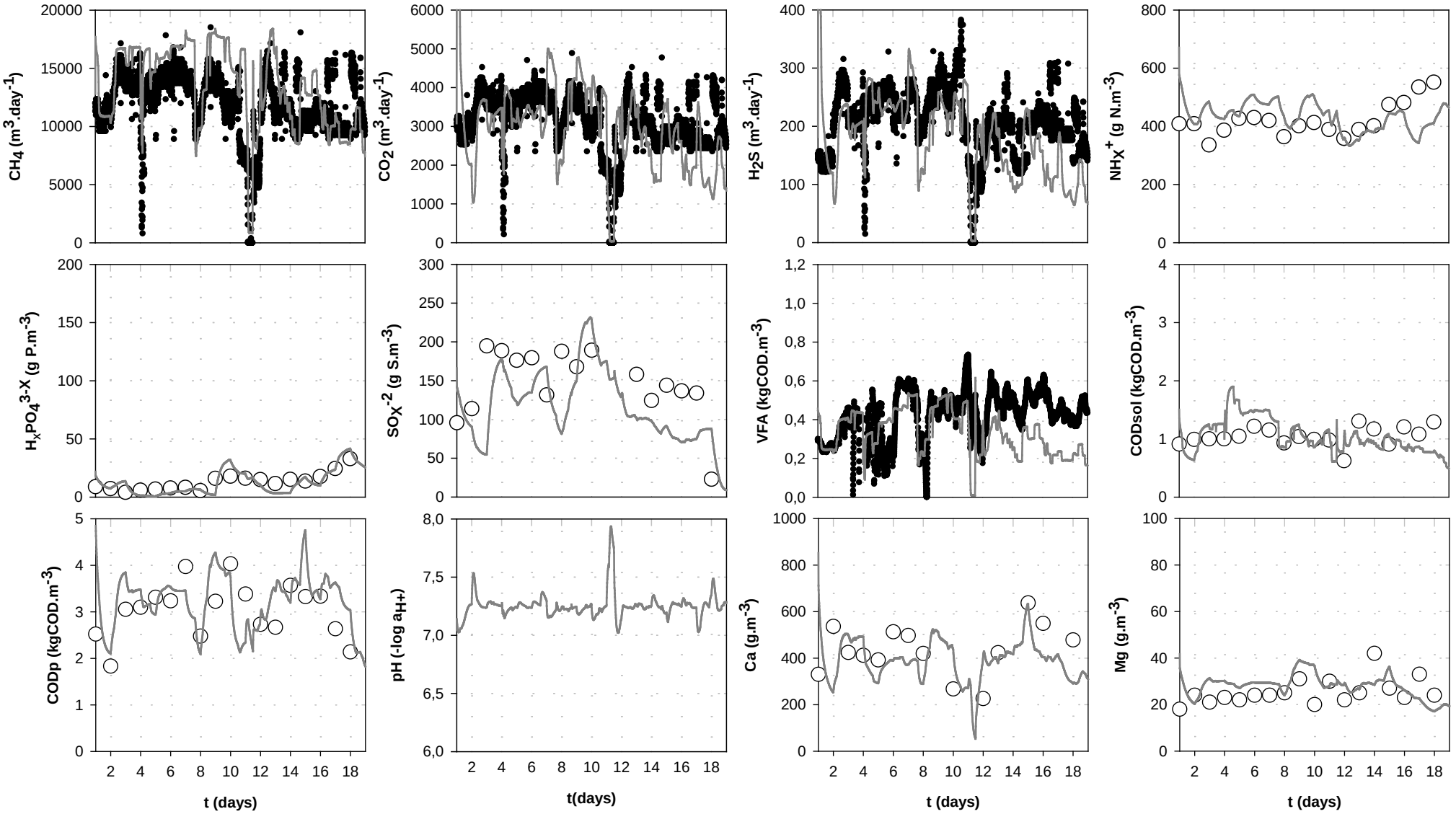

Figure 4. Simulation results and measured effluent data for data set 2 (#*D*2).

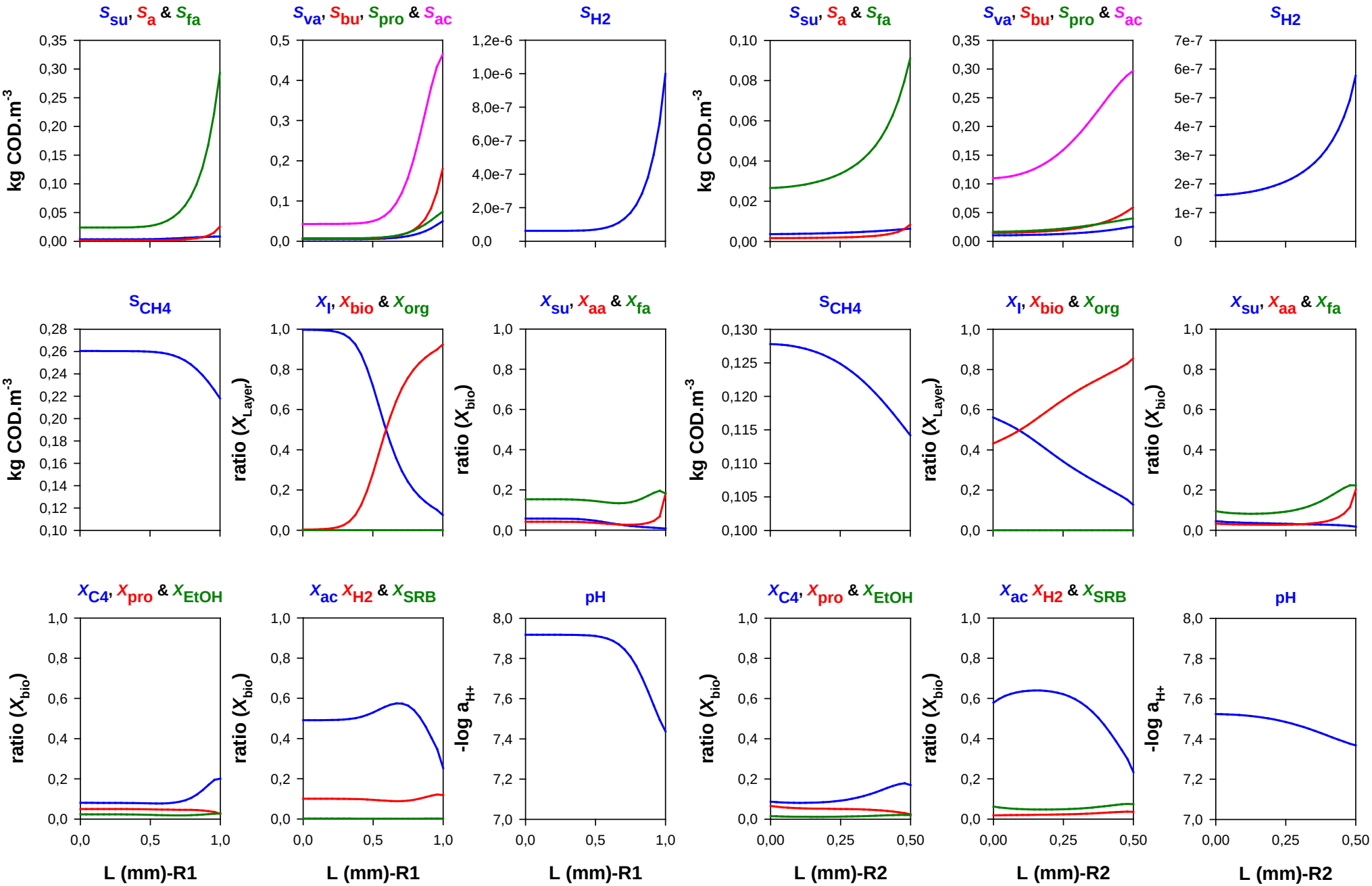

Figure 5. Predicted biomass/organics/pH distribution within the biofilm in the lower (*R*1) (columns 1,2,3) and upper (*R*2) (columns 4,5,6) parts of the bioreactor for data set 1 (#D1). 0.000 = centre. X_{Layer} and X_{bio} are total particulates and biomass per each discretized layer. Organics, inerts and biomass are displayed in relative terms.

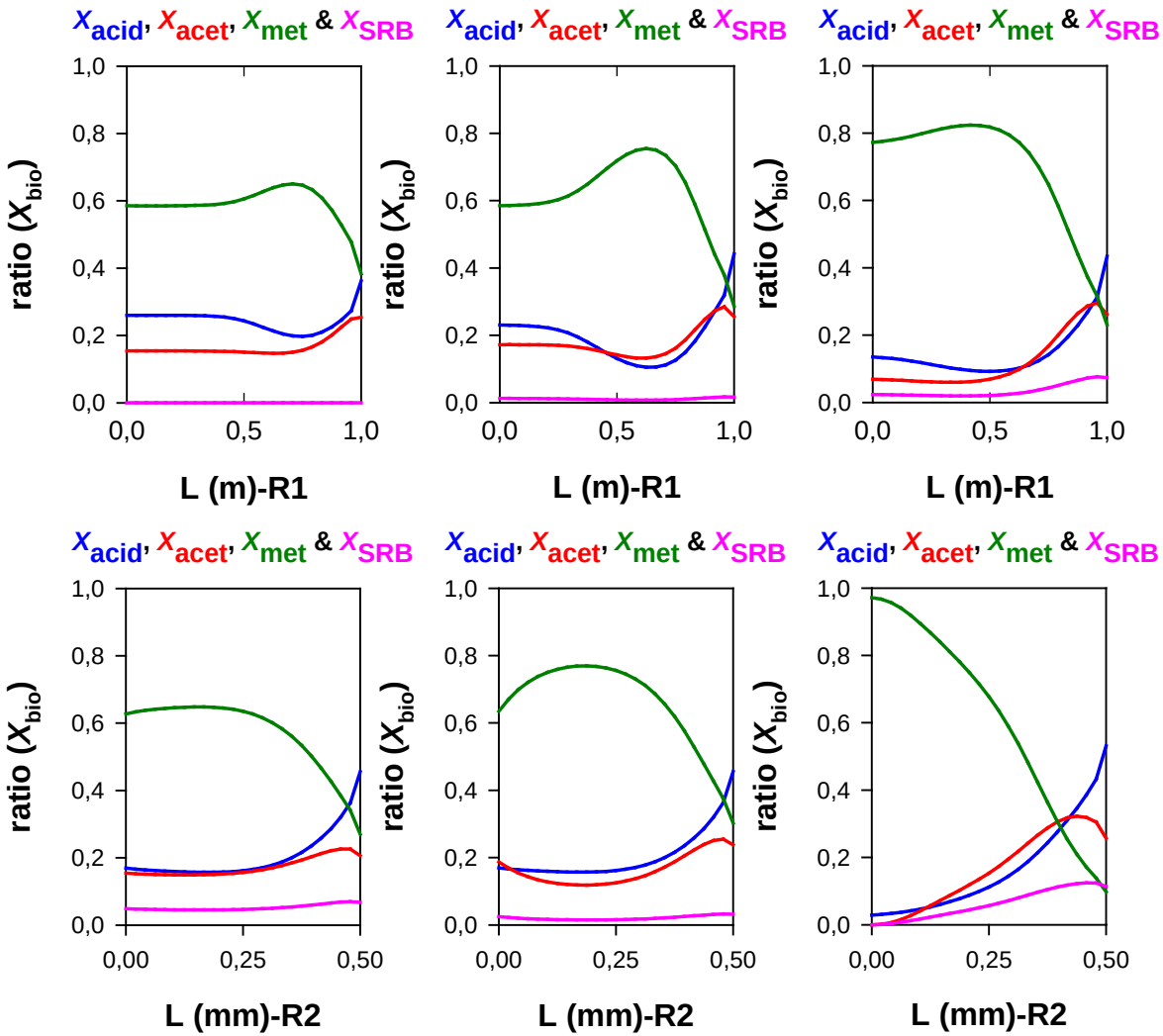

Figure 6. Predicted biomass distributions in the granules under three different conditions: default operational conditions (column 1), pH decrease (column 2) and higher S loads (column 3). #*D*1 is used to run the simulations. $X_{acid} = X_{su} + X_{aa} + X_{fa}$ // $X_{acet} = X_{C4} + X_{pro} + X_{EtOH}$ // $X_{met} = X_{H2} + X_{ac.}$. Biomass is displayed in relative terms.

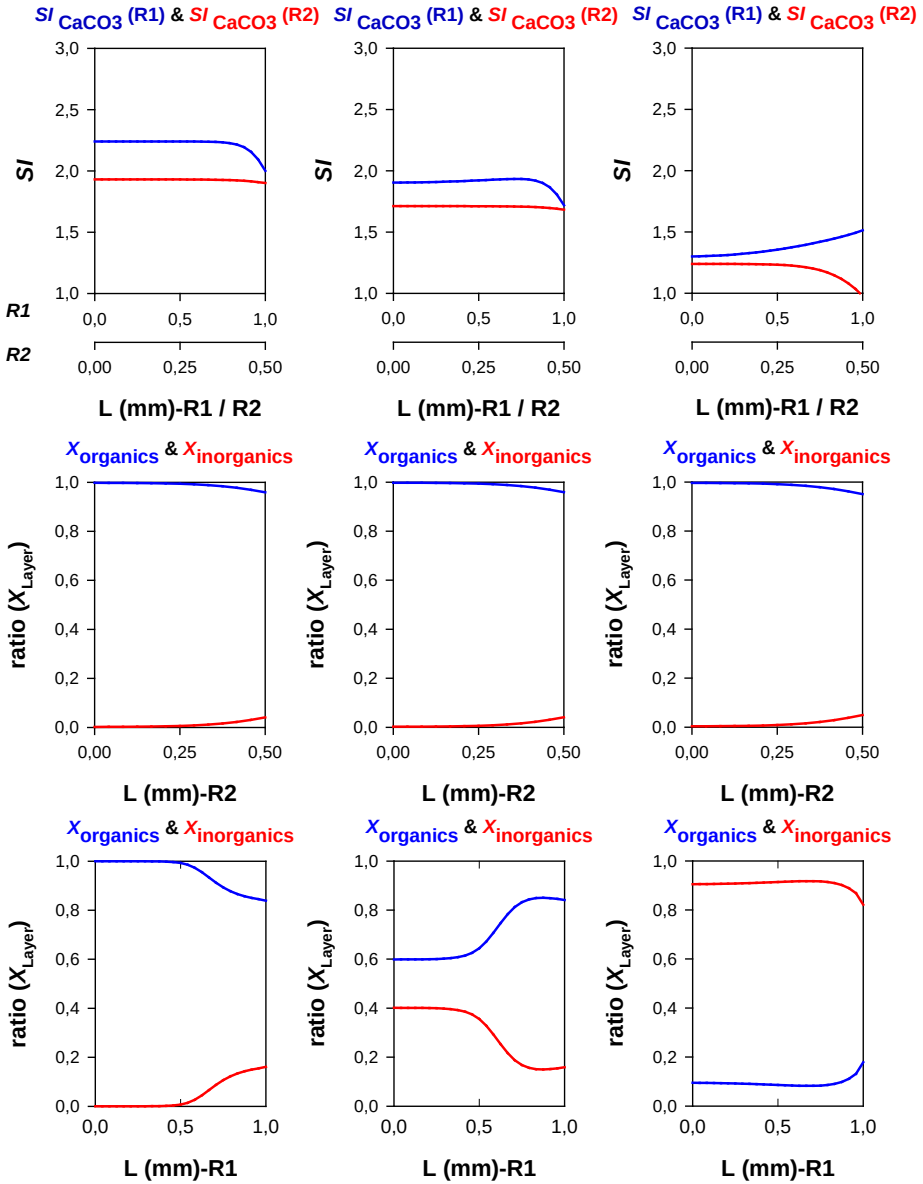

Figure 7. *SI* values (row 1) and granular distributions of organic and inorganic material (rows 2, 3) for *R*1 and *R*2 using data set 2 (#*D*2). Simulation times are 0 days (column 1, initial distribution), 25 days (column 2) and 50 days (column 3). Inorganics and organics are displayed in relative terms.

RESEARCH HIGHLIGHTS

- A multi-scale model describing an anaerobic digestion process is constructed.
- The model behaviour is analysed using two different industrial (full scale) data sets.
- The model successfully predicts COD, N, P, S, pH and mineral behaviour.
- Scenario analysis shows the effect of changing the operational conditions in both bulk and biofilm.